

# Footprint biometric authentication using SqueezeNet

Sairul Izwan Safie, Rusmawarni Ramli

Malaysian Institute of Industrial Technology, Universiti Kuala Lumpur, Johor Bahru, Malaysia

## Article Info

### Article history:

Received Jul 20, 2022

Revised Apr 11, 2023

Accepted Apr 16, 2023

### Keywords:

Authentication

Biometric

Convolutional neural network

Footprints

SqueezeNet

## ABSTRACT

Biometric authentication is a process of identity verification once an identity is claimed by an individual. It uses unique features on the human body. Footprints are a new biometric feature that has sparked interest among researchers, as this feature is universal, easy to extract and has not changed throughout time. The focus of researchers in this field is to improve the recognition rate. Various techniques have been developed for this purpose, but the accuracy percentage is at 98% with an equal error rate (EER) of 6.1%. This paper proposes the use of a new technique called SqueezeNet in classifying footprint images. SqueezeNet belongs to the convolutional neural network (CNN) family. In this study, 300 footprint images were used from 15 individuals. The 70% of these images were used to train the proposed SqueezeNet network, while the rest were used for testing. At the end of this simulation, SqueezeNet has achieved an accuracy of 98.67% with an EER of 2.1%.

*This is an open access article under the [CC BY-SA](https://creativecommons.org/licenses/by-sa/4.0/) license.*



## Corresponding Author:

Sairul Izwan Safie

Malaysian Institute of Industrial Technology, Universiti Kuala Lumpur

Johor Bahru, Johor, Malaysia

Email: sairulizwan@unikl.edu.my

## 1. INTRODUCTION

Biometric systems can work either in authentication or identification mode. Traditionally, for a biometric system to operate in authentication mode, an individual must first claim an identity stored in a database. Username and smart card are two examples of how identity can be claimed from a system. Next, the system will find the feature vector stored based on the information of the claimed identity. The claimer is then required to submit their biometrics as a test sample before its feature vector is extracted. The system will eventually make a comparison between the newly extracted and stored features to determine whether the claim is valid or a fraud [1]. Compared to the identification mode, for which the system is required to determine whether the claimer is part of the individuals registered in the system.

The past decade has seen an increase in using footprints for biometric authentication. Footprints are universal, easy to retrieve and have not changed much throughout time [2]. Using footprints for biometrics is not as extensive as other biometric traits, yet it still has its own applications. In the 19<sup>th</sup> century, the use of footprints had been used as a biometric identity for newborns [3]. The footprints of this newborn will be stamped on a piece of paper and kept in the hospital. In the 21<sup>st</sup> century, the use of these footprints has been replaced by tags or radio frequency identification (RFID). However, it can only be used while the baby is still in the hospital. After the baby was discharged, no self-identification system followed them [4]. This is where the use of footprints can be fully used again. To combat crime, footprints are also often used as evidence in court. Criminals often leave traces of shoes or footprints on the scene [5]. Footprints-based biometric authentication systems are useful in such situations. In terms of security systems, footprints are ideal for use as personal authentication systems, especially applications that have small databases. In most Asian countries such as Japan and Malaysia, it is customary to take off shoes before entering the house [6]. A footprint-based

biometric authentication system can be used here by placing a scanner to open the door. When the footprint on the scanner is genuine, as listed in the database, then the door will open.

Images used for footprint-based recognition can be categorized into static [7] and dynamic [8]. To get a static image, an individual must stand in a fixed position before the image of his or her foot is captured. Dynamic images are taken while an individual is walking. Various techniques have been used to extract the characteristics of the footprints for matching purposes. Nakajima *et al.* [7] used the normalized static footprint images for recognition and got 85% accuracy. Eigenfeet, ballprint and foot geometry techniques have been used in [9] for person identification and achieved 97% recognition rate for 16 subjects. Krishan *et al.* [10] used foot outline geometry on 1040 male Gujar subjects to estimate stature from footprint. Similar technique is used in [11] on 400 adult Malaysian Malay. In both studies, manual geometry features are extracted from the footprint. dynamic time warping (DTW), along with the distance between the contour point and its center, was used as a footprint feature in [12]. In 600 samples, 455 are successfully classified correctly.

Non-geometric features have also been implemented for footprint recognition, either using footprint images or taken from the sensor. The hidden Markov model (HMM), combined with the Levenberg-Marquart learning method, was applied on a pressure mat to classify footprints [8]. This study used 11 samples and 80% of them were correctly recognized. Fuzzy logic-based solutions have also been applied to load distribution sensors for footprint recognition [13]. The study was conducted on 30 subjects and achieved 6.1% equal error rate (EER). A wavelet -based feature known as modified sequential haar energy (MSHE) was applied in [14] to classify footprint images from 400 individuals. They achieved a 92% recognition rate in their study. In other works, Kumar *et al.* [15] proposed the used of principal component analysis (PCA) features and achieved 93% recognition rate. Recently, deep learning techniques have been used as footprint biometric identification for children [4]. In that study, a crease patterns of the footprint images are used as the input to the convolutional neural network (CNN). The 48 subjects were used in the study, and they achieved 98% recognition rate.

In this paper, we propose the use of SqueezeNet to classify individuals using footprint images. SqueezeNet is one of CNN's architectures created by Iandola *et al.* [16]. Several changes were made to this architecture for our system, and these are described in section 2. Section 2 also describes how training and test databases are constructed in our simulations. Section 3 presents the performance of the proposed system. Section 4 concludes the paper.

## 2. METHOD

### 2.1. Convolutional neural network

The convolutional neural networks (CNN) is a powerful deep learning architecture that includes an input layer, stacked pairs of convolutional and pooling layers, a fully connected layer, and an output layer, as depicted in Figure 1 [17]. The neurons in each layer are arranged as height, width, and depth (channel). Using CNN in image processing allows features to be extracted automatically and avoids the use of manually designed input features [18].

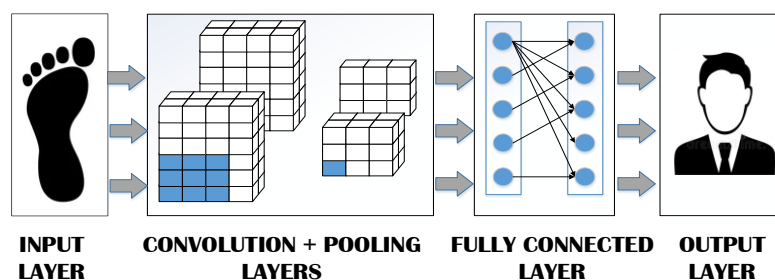


Figure 1. Convolutional neural networks (CNN)

The input data for the CNN is typically structured in the form of a grid with multiple channels, allowing for the preservation of strong spatial dependencies within local grid are [19]. The convolution layer plays a crucial role in extracting discriminative features from the input data by applying learned weights to connectors. CNN employs multiple channels, each capturing different aspects of the previous layer. Convolution offers several advantages, including weight sharing and translation invariance [20]. Filters, usually of odd sizes like  $3 \times 3$  or  $5 \times 5$ , are used in the convolution layer to generate new data feature maps. These filters move across the input data or feature map, scanning from top to bottom and left to right with a specific

'Stride' value, while taking into account any padding that may have been applied. Padding adds blank or empty pixels to the edges of the data frame to aid in preserving the spatial dimensions during convolution.

Assume that the dimensions of the filter in the  $q^{th}$  layer is in the size of  $F_q \times F_q$ . Let the  $p^{th}$  filter in layer  $q$  be denoted by a 2-dimensional matrix  $W^{[p,q]} = [\omega_{ij}^{[p,q]}]$ . The indices  $i$  and  $j$  are the height and width of the filter. The feature map in layer  $q$  is represented by a 2-dimensional matrix  $H^{[q]} = [h_{ij}^{[q]}]$ . Mathematically, the convolution operation in the convolution layer from layer  $q$  to layer  $(q+1)$  can be described as shown in (1).

$$h_{ijp}^{(q+1)} = \sum_{r=1}^{F_q} \sum_{s=1}^{F_q} \omega_{rs}^{(p,q)} h_{i+r-1, j+s-1}^{(q)} \tag{1}$$

To ensure that the system is in a state of nonlinearity, the rectified linear unit (ReLU) is used immediately after the convolution layer described in (1). The ReLU converts all negative activations to 0 using the function  $f(y) = \max(0, y)$  [21]. The adjacent data generated after the convolution layer is then combined into one representative value using the pooling layer. These neighborhood data are selected in the same rectangular size. The pooling process is done sequentially from left to right and top to bottom according to the number of 'Strides' throughout the images. Typically, representative values for a selected set of data are set using either the average or maximum mode. After passing through the convolution and pooling layers as shown in Figure 1, the data is then fed into the fully connected layer for classification of the state of each input frame. The fully connected layer follows a standard deep neural network architecture, leading to the output layer. A softmax classifier is commonly used to make predictions based on the output of the network.

**2.2. SqueezeNet**

SqueezeNet was built based on the CNN concept, with a few modifications. For SqueezeNet, the elements in the convolution and pooling layers shown in Figure 1 are mostly replaced with fire module blocks [22]. A fire module comprises squeeze and expand layers, as shown in Figure 2.

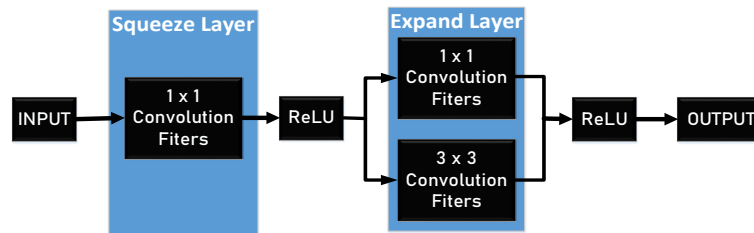


Figure 2. Fire module

The ReLU activation function is also used between these layers to increase the network depth [23]. The squeeze layer contains only a  $1 \times 1$  convolution filters, while the expand layer has a concatenation of  $1 \times 1$  and  $3 \times 3$  convolution filters. SqueezeNet also does not use fully connected layers, as shown in Figure 1. Several modifications have been made to the original structure of SqueezeNet, proposed by Iandola *et al.* [16] in terms of SqueezeNet layer's location, as shown in Figure 3. In Figure 3, the terms 'conv', 'pool' and 'fire' respectively represent the convolution, pooling, and fire module layers. As seen in Figure 3, it can be concluded that the SqueezeNet was built using 2 convolution layers, 3 maximum pooling layers, and 8 fire module layers. In most networks, the last layer with learnable weights is a fully connected layer. For SqueezeNet, the last learnable layer is the final convolutional layer combined with the global average pool and Softmax activation function. This configuration allows SqueezeNet to be highly accurate with a small size model [24]. It makes SqueezeNet an option in biometric systems, because of the short use of time for feature extraction and recognition processes.

**2.3. Simulation setup**

In this study, the object of interest is footprint images. All participants' footprint images were recorded using an Apple iPhone 11 Pro, which was positioned at a distance of 50 cm from the participant, as depicted in Figure 4. A white plain wood was used as the background during the image recording session to ensure that the captured images had invariant characteristics throughout the experiment. Fifteen candidates, aged between 20 and 25 years old, volunteered to participate in this research. Each participant contributed 10 images of both their left and right footprints in 10 separate sessions, resulting in a total of 300 footprint images used in this

study. The size of the images captured by the Apple iPhone 11 was  $670 \times 372 \times 3$ , which was then resized to  $227 \times 227 \times 3$  to comply with the SqueezeNet architecture requirements. The footprint image database was divided into 70% for training data and 30% for validation data.

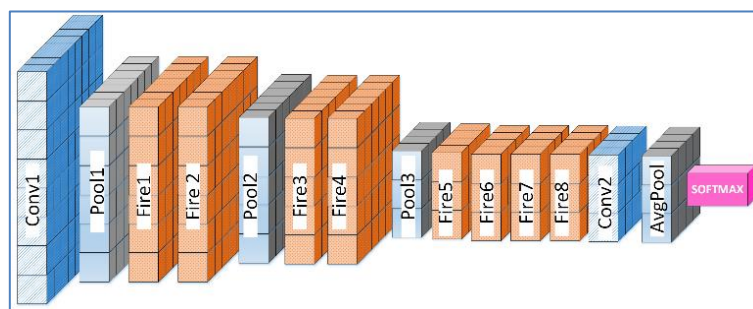


Figure 3. SqueezeNet



Figure 4. Footprint image capturing process

The SqueezeNet models are trained using the stochastic gradient descent with momentum (SGDM) optimizer algorithm [25]. Batch learning is employed, updating the model every 10 sets of data, and the training process is limited to a maximum of 20 epochs. The initial learning rate is set to 0.0003.

### 3. RESULTS AND DISCUSSION

This section discusses the results of using SqueezeNet for footprint biometric authentication. SqueezeNet will be analyzed visually to see the computational cost using this network. We will also discuss recognition results and variables that affect network accuracy.

#### 3.1. Network analysis

Table 1 shows a detailed description of each proposed SqueezeNet. In layers with reference to Figure 3 that has been used in this paper. As seen from Table 1, there are 1,200,000 learnable weights and biases need to be updated for each epoch of the training process.

#### 3.2. Network training and validation

The proposed SqueezeNet network has used the initial values of weights and biases, based on a pre-training version of the SqueezeNet that has been performed on more than a million images from the ImageNet database [26]. This pre-training network has been used to classify images into 1,000 categories of objects and further used in this project. Figure 5 shows the training accuracy of the proposed network using the footprint training data. As seen from the figure, the final validation accuracy obtained after 20 epochs is 98.67% when the test (validation) data is used. It took approximately 5 minutes to train and test all images. The network achieves validation accuracy greater than 90% starting from the 10<sup>th</sup> epoch (200<sup>th</sup> iteration). Figure 6 shows the training loss of the proposed network. As seen from the figure, the final training loss for the network is 0.09%. The training loss is less than 1% from the 8<sup>th</sup> epoch (160<sup>th</sup> iteration).

Table 1. Network analysis of SqueezeNet

Layer	Type	Filter			Output size	Learnable properties	
		No	Size	Stride		Weight	Bias
Input	Image input				227x227x3		
Conv1	Convolution	64	3x3x3	2	113x113x64	3x3x3x64	1x1x64
Pool1	Max pooling		3x3	2	56x56x64		
Fire1	Fire: Squeeze	16	1x1x64	1	56x56x16	1x1x64x16	1x1x16
	Fire: Expand [1x1]	64	1x1x16	1	56x56x64	1x1x16x64	1x1x64
	Fire: Expand [3x3]	64	3x3x16	1	56x56x64	3x3x16x64	1x1x64
	Fire: Concatenation				56x56x128		
Fire2	Fire: Squeeze	16	1x1x128	1	56x56x16	1x1x128x16	1x1x16
	Fire: Expand [1x1]	64	1x1x16	1	56x56x64	1x1x16x64	1x1x64
	Fire: Expand [3x3]	64	3x3x16	1	56x56x64	3x3x16x64	1x1x64
	Fire: Concatenation				56x56x128		
Pool2	Max Pooling		3x3	2	28x28x128		
Fire3	Fire: Squeeze	32	1x1x128	1	28x28x32	1x1x128x32	1x1x32
	Fire: Expand [1x1]	128	1x1x32	1	28x28x128	1x1x32x128	1x1x128
	Fire: Expand [3x3]	128	3x3x32	1	28x2x128	3x3x32x128	1x1x128
	Fire: Concatenation				28x28x256		
Fire4	Fire: Squeeze	32	1x1x256	1	28x28x32	1x1x256x32	1x1x32
	Fire: Expand [1x1]	128	1x1x32	1	28x28x128	1x1x32x128	1x1x128
	Fire: Expand [3x3]	128	3x3x32	1	28x28x128	3x3x32x128	1x1x128
	Fire: Concatenation				28x28x256		
Pool3	Max Pooling		3x3	2	14x14x256		
Fire5	Fire: Squeeze	48	1x1x256	1	14x14x48	1x1x256x48	1x1x48
	Fire: Expand [1x1]	192	1x1x48	1	14x14x192	1x1x48x192	1x1x192
	Fire: Expand [3x3]	192	3x3x48	1	14x14x192	3x3x48x192	1x1x192
	Fire: Concatenation				14x14x384		
Fire6	Fire: Squeeze	48	1x1x384	1	14x14x48	1x1x384x48	1x1x48
	Fire: Expand [1x1]	192	1x1x48	1	14x14x192	1x1x48x192	1x1x192
	Fire: Expand [3x3]	192	3x3x48	1	14x14x192	3x3x48x192	1x1x192
	Fire: Concatenation				14x14x384		
Fire7	Fire: Squeeze	64	1x1x384	1	14x14x64	1x1x384x64	1x1x64
	Fire: Expand [1x1]	256	1x1x64	1	14x14x256	1x1x64x256	1x1x256
	Fire: Expand [3x3]	256	3x3x64	1	14x14x256	3x3x64x256	1x1x256
	Fire: Concatenation				14x14x512		
Fire8	Fire: Squeeze	64	1x1x512	1	14x14x64	1x1x512x64	1x1x64
	Fire: Expand [1x1]	256	1x1x64	1	14x14x256	1x1x64x256	1x1x256
	Fire: Expand [3x3]	256	3x3x64	1	14x14x256	3x3x64x256	1x1x256
	Fire: Concatenation				14x14x512		
Conv2	Convolution	30	1x1x512	2	14x14x30	1x1x512x30	1x1x30

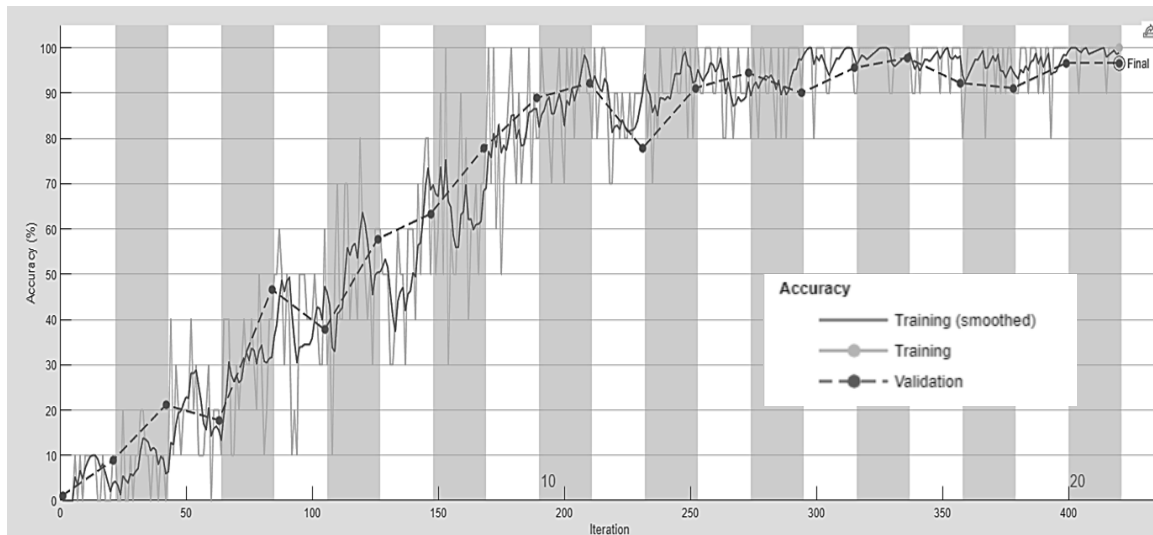


Figure 5. Training accuracy

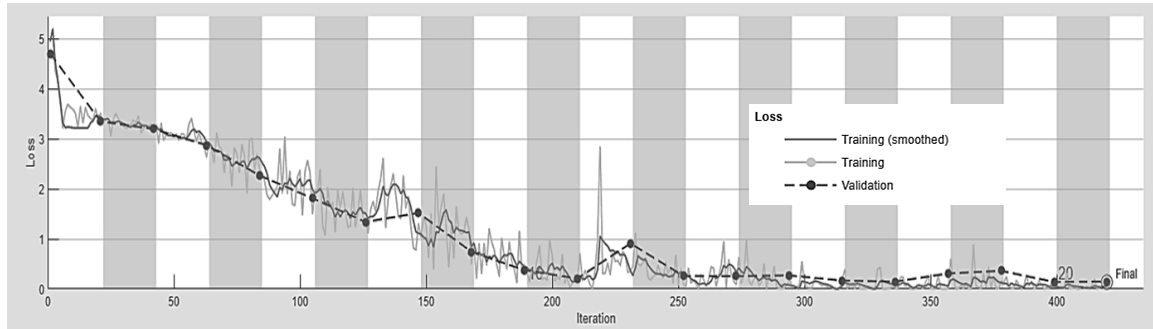


Figure 6. Training loss

### 3.3. Confusion matrix

We tested the accuracy of the proposed SqueezeNet architecture using the test database that had been developed. This time, the test data was divided into left and right footprint categories. We used the confusion matrix as shown in Figure 7 and Figure 8 to represent the accuracy of our network. Figure 7 illustrates the accuracy of classifying individuals using left footprint images. As shown in Figure 7, only 1 image out of 3 of the left footprint of the subject ‘FTP07L’ was mis-classified to ‘FTP06L’. For the rest, the proposed SqueezeNet network classified them all correctly. When the right foot was used to identify an individual, these footprint images were successfully classified all images correctly. This is shown in Figure 8.

### 3.4. Equal error rate

Among the important measures to evaluate the performance of biometric systems are the true positive rate (TPR) and the false positive rate (FPR). TPR measures the probability that a genuine classification classified by the system is coming from a genuine individual. FPR measures the probability that the genuine classification shown by the system is from the impostor. To simulate these results, we trained the left and right footprint images separately using the proposed network. The proposed network that had been trained using the left footprint images was used to classify individuals using the right footprint images, and vice versa. The results of TPR versus FPR are presented as the receiver operating characteristic (ROC) curve, shown in Figure 9. From Figure 9, it is observed that the proposed system generates 0.23 equal error rate (EER), i.e., the point at which FPR is equivalent to 1-TPR. The ROC curve also allows the performance of the proposed system to be compared with other systems under different parameter settings [27]. It is measured using the area under the ROC curve (AUC) value. The system we proposed gives a value of 0.86 for AUC.

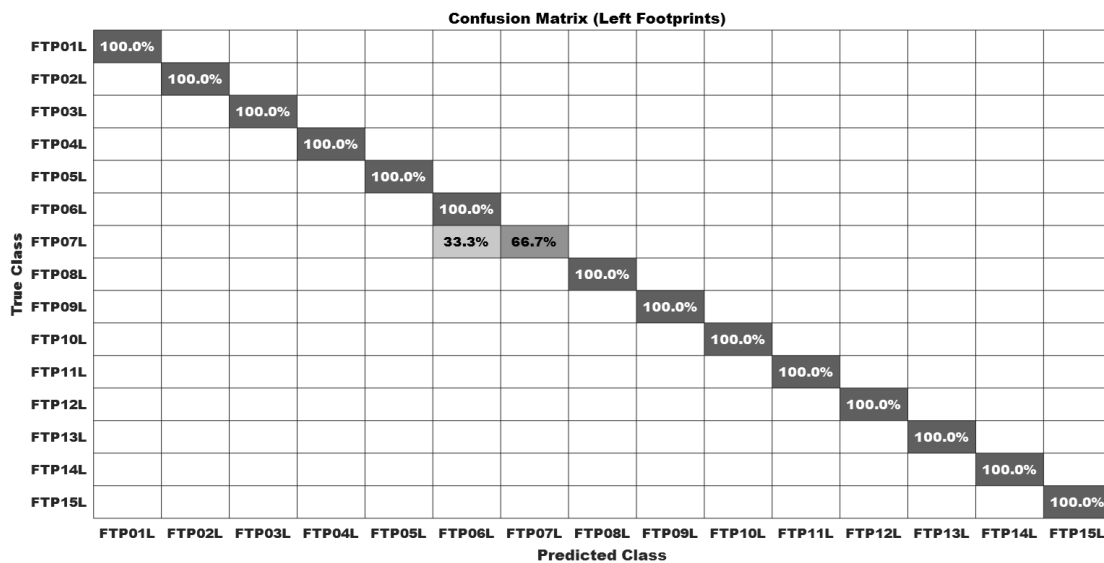


Figure 7. Confusion matrix for left footprints authentication

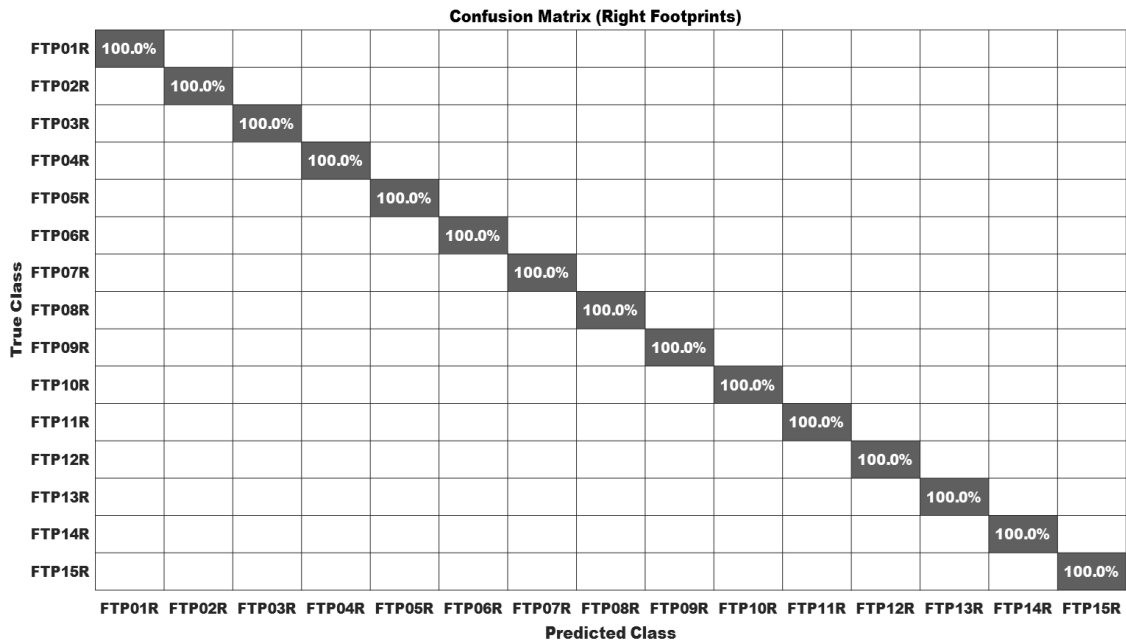


Figure 8. Confusion matrix for right footprints authentication

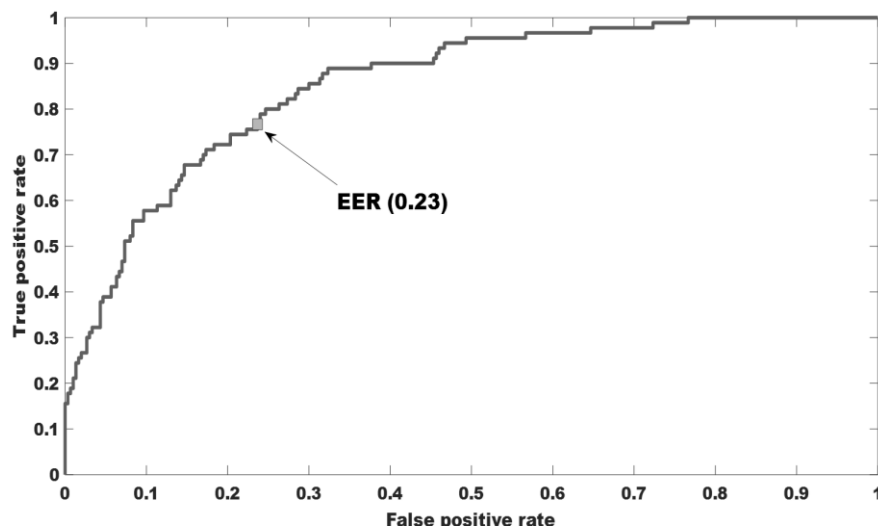


Figure 9. Receiver operating characteristic (ROC) curve

#### 4. CONCLUSION

Footprint-based biometric authentication has garnered attention in the field of biometrics, and various methods have been proposed to improve accuracy. In this study, we investigated the use of the SqueezeNet technique for enhanced recognition accuracy. Unlike previous methods, our approach eliminates the need for hand-crafted feature extraction prior to classification. Performance evaluation was based on the confusion matrix and ROC curve, using a dataset of 300 images for training and testing. Our simulation showed that the proposed network achieved an accuracy of 98.67% and an EER of 2.1%, representing an improvement of approximately 1% compared to the state-of-the-art technique reported in the literature. Furthermore, our results revealed that right footprints outperformed left footprints in terms of correct classification within the scope of our developed databases, a finding that has received limited discussion in previous research. The small size of the deep learning architecture, with only 1,200,000 learning parameters to update during training, makes it suitable for practical biometric hardware adaptation.

## REFERENCES

- [1] S. I. Safie, J. J. Soraghan, and L. Petropoulakis, "Electrocardiogram (ECG) biometric authentication using pulse active ratio (PAR)," *IEEE Transactions on Information Forensics and Security*, vol. 6, no. 4, pp. 1315–1322, Dec. 2011, doi: 10.1109/TIFS.2011.2162408.
- [2] D. P. Nguyen, C. B. Phan, and S. Koo, "Predicting body movements for person identification under different walking conditions," *Forensic Science International*, vol. 290, pp. 303–309, Sep. 2018, doi: 10.1016/j.forsciint.2018.07.022.
- [3] J. Kotzerke, S. A. Davis, J. McVernon, and K. J. Horadam, "Steps to solving the infant biometric problem with ridge-based biometrics," *IET Biometrics*, vol. 7, no. 6, pp. 567–572, Nov. 2018, doi: 10.1049/iet-bmt.2017.0282.
- [4] V. Kamble and M. Dale, "Deep Learning for Biometric Recognition of Children using Footprints," in *2022 International Conference on Emerging Smart Computing and Informatics, ESCI 2022*, Mar. 2022, pp. 1–6, doi: 10.1109/ESCI53509.2022.9758315.
- [5] A. Shukla, A. Katal, S. Raghuvanshi, and S. Sharma, "Criminal combat: Crime analysis and prediction using machine learning," in *2021 International Conference on Intelligent Technologies, CONIT 2021*, Jun. 2021, pp. 1–5, doi: 10.1109/CONIT51480.2021.9498397.
- [6] T. Murachi, "Taking off shoes to enter Japanese houses—why?," *Perspectives in Biology and Medicine*, vol. 32, no. 3, pp. 385–386, 1989, doi: 10.1353/pbm.1989.0046.
- [7] K. Nakajima, Y. Mizukami, K. Tanaka, and T. Tamura, "Footprint-based personal recognition," *IEEE Transactions on Biomedical Engineering*, vol. 47, no. 11, pp. 1534–1537, 2000, doi: 10.1109/10.880106.
- [8] J. W. Jung, Z. Bien, S. W. Lee, and T. Sato, "Dynamic-Footprint based Person Identification using Mat-type Pressure Sensor," in *Annual International Conference of the IEEE Engineering in Medicine and Biology - Proceedings*, 2003, vol. 3, pp. 2937–2940, doi: 10.1109/iembs.2003.1280533.
- [9] A. Uhl and P. Wild, "Personal identification using Eigenfeet, Ballprint and Foot geometry biometrics," in *IEEE Conference on Biometrics: Theory, Applications and Systems, BTAS '07*, Sep. 2007, pp. 1–6, doi: 10.1109/BTAS.2007.4401924.
- [10] K. Krishan, "Estimation of stature from footprint and foot outline dimensions in Gujjars of North India," *Forensic Science International*, vol. 175, no. 2–3, pp. 93–101, Mar. 2008, doi: 10.1016/j.forsciint.2007.05.014.
- [11] T. N. Moorthy and S. F. B. Sulaiman, "Individualizing characteristics of footprints in Malaysian Malays for person identification from a forensic perspective," *Egyptian Journal of Forensic Sciences*, vol. 5, no. 1, pp. 13–22, Mar. 2015, doi: 10.1016/j.ejfs.2014.04.003.
- [12] R. Kushwaha, N. Nain, and G. Singal, "Detailed analysis of footprint geometry for person identification," in *Proceedings - 13th International Conference on Signal-Image Technology and Internet-Based Systems, SITIS 2017*, Dec. 2018, vol. 2018-January, pp. 229–236, doi: 10.1109/SITIS.2017.47.
- [13] T. Takeda, K. Taniguchi, K. Asari, K. Kuramoto, S. Kobashi, and Y. Hata, "Biometric personal authentication by one step foot pressure distribution change by load distribution sensor," in *IEEE International Conference on Fuzzy Systems*, Aug. 2009, pp. 906–910, doi: 10.1109/FUZZY.2009.5277149.
- [14] V. D. A. Kumar and M. Ramakrishan, "Footprint based recognition system," in *Communications in Computer and Information Science*, vol. 147 CCIS, 2011, pp. 358–367.
- [15] V. D. A. Kumar, V. D. A. Kumar, S. Malathi, and P. Jagadeesh, "Intruder identification using footprint recognition with PCA and SVM classifiers," *Advanced Materials Research*, vol. 984–985, pp. 1345–1349, Jul. 2014, doi: 10.4028/www.scientific.net/AMR.984-985.1345.
- [16] F. N. Iandola, S. Han, M. W. Moskewicz, K. Ashraf, W. J. Dally, and K. Keutzer, "SqueezeNet: AlexNet-level accuracy with 50x fewer parameters and <0.5MB model size," *arXiv preprints*, Feb. 2016, [Online]. Available: <http://arxiv.org/abs/1602.07360>.
- [17] I. S. Safie, R. Ramli, M. A. Azri, M. Aliff, and Z. Mohamad, "Raspberry Pi based driver drowsiness detection system using convolutional neural network (CNN)," in *2022 IEEE 18th International Colloquium on Signal Processing and Applications, CSPA 2022 - Proceeding*, May 2022, pp. 30–34, doi: 10.1109/CSPA55076.2022.9781879.
- [18] T. Chai, S. Prasad, J. Yan, and Z. Zhang, "Contactless palmprint biometrics using DeepNet with dedicated assistant layers," *Visual Computer*, Jul. 2022, doi: 10.1007/s00371-022-02571-6.
- [19] F. Li, J. Feng, H. Yan, D. Jin, and Y. Li, "Crowd flow prediction for irregular regions with semantic graph attention network," *ACM Transactions on Intelligent Systems and Technology*, vol. 13, no. 5, pp. 1–14, Oct. 2022, doi: 10.1145/3501805.
- [20] I. W. Selesnick, R. G. Baraniuk, and N. G. Kingsbury, "The dual-tree complex wavelet transform," *IEEE Signal Processing Magazine*, vol. 22, no. 6, pp. 123–151, Nov. 2005, doi: 10.1109/MSP.2005.1550194.
- [21] M. Varshney and P. Singh, "Optimizing nonlinear activation function for convolutional neural networks," *Signal, Image and Video Processing*, vol. 15, no. 6, pp. 1323–1330, Sep. 2021, doi: 10.1007/s11760-021-01863-z.
- [22] B. Qiang *et al.*, "SqueezeNet and fusion network-based accurate fast fully convolutional network for hand detection and gesture recognition," *IEEE Access*, vol. 9, pp. 77661–77674, 2021, doi: 10.1109/ACCESS.2021.3079337.
- [23] Y. Yu, K. Adu, N. Tashi, P. Anokye, X. Wang, and M. A. Ayidzoe, "RMAF: Relu-Memristor-Like Activation Function for Deep Learning," *IEEE Access*, vol. 8, pp. 72727–72741, 2020, doi: 10.1109/ACCESS.2020.2987829.
- [24] J. Zhang, H. Zhu, P. Wang, and X. Ling, "ATT Squeeze U-Net: A Lightweight Network for Forest Fire Detection and Recognition," *IEEE Access*, vol. 9, pp. 10858–10870, 2021, doi: 10.1109/ACCESS.2021.3050628.
- [25] S. Postalçloğlu, "Performance analysis of different optimizers for deep learning-based image recognition," *International Journal of Pattern Recognition and Artificial Intelligence*, vol. 34, no. 2, p. 2051003, Feb. 2020, doi: 10.1142/S0218001420510039.
- [26] O. Russakovsky *et al.*, "ImageNet large scale visual recognition challenge," *International Journal of Computer Vision*, vol. 115, no. 3, pp. 211–252, Dec. 2015, doi: 10.1007/s11263-015-0816-y.
- [27] S. I. Safie, P. Z. M. Khalid, and M. Aimullah, "Modeling phasmophobia (fear of ghosts) using electroencephalogram," *Indonesian Journal of Electrical Engineering and Computer Science*, vol. 26, no. 2, pp. 743–753, May 2022, doi: 10.11591/ijeecs.v26.i2.pp743-753.

**BIOGRAPHIES OF AUTHORS**

**Sairul Izwan Safie**    received the Bach of Engineering (Electrical) and Master of Electrical Engineering (Power) from the Universiti Teknologi Malaysia. Received his Ph.D. degree in electronic and electrical engineering from the University of Strathclyde, Glasgow, United Kingdom. He is currently an Associate Professor of Universiti Kuala Lumpur-Malaysian Institute of Industrial Technology. His research interest is in artificial intelligence, big data, signal, and image processing with application to biometric, psychological, and physiological signal, image, and video processing). He can be contacted at email: [sairulizwan@unikl.edu.my](mailto:sairulizwan@unikl.edu.my).



**Rusmawarni Ramli**    holds a Bachelor of Engineering (B. Eng Chemical), Master in Engineering (M.Eng. Bioprocess), Professional certificates in Chemical Technology by Malaysia Board of Technologist (MBOT) and member of Graduate Engineer by Board of Engineers Malaysia (BEM). She is currently lecturing with the Instrumentation and Control Engineering Department. Her research areas of interest include Bioprocess, Process Control, enzyme Purification and Design optimization. She can be contacted at email: [rusmawarni@unikl.edu.my](mailto:rusmawarni@unikl.edu.my).